Journal of Nuclear Materials 392 (2009) 413–419

Contents lists available at ScienceDirect

Journal of Nuclear Materials

journal homepage: www.elsevier.com/locate/jnucmat

# Helium bubbles formation in aluminum: Bulk diffusion and near-surface diffusion using TEM observations

Benny Glam [a,b,*], Shalom Eliezer [a], Daniel Moreno [a], Dan Eliezer [b]

[a] Soreq Nuclear Research Center, Propulsion Physics, Yavne 81800, Israel
[b] Ben-Gurion University of the Negev, Materials Engineering Department, Beer-Sheva, Israel

ARTICLE INFO

*Article history:*
Received 17 December 2008
Accepted 31 March 2009

ABSTRACT

Experimental and analytical investigation of helium bubble formation and growth in aluminum is presented. A pure aluminum with 0.15 wt% of $^{10}B$ was neutron-irradiated in the Soreq nuclear reactor to get homogeneous helium atoms in the metal according to the reaction $^{10}B + n \rightarrow {}^{7}Li + {}^{4}He$. Formation and growth of helium bubbles was observed in situ by heating the post-irradiated metal to 470 °C in TEM with a hot stage holder. It was found that above 400 °C the change in the bubble shape takes less than a second. In other experiments the Al–$^{10}B$ was first heated in its bulk shape and then observed in TEM at room temperature. In this case the helium bubble formation takes hours. Analytical evaluation of the diffusion processes in both cases was done to explain the experimental results. The number of helium atoms in a bubble was calculated from the electron energy loss spectrum (EELS) measurements. These measurements confirmed the hard sphere equation of state (EOS) for inert gases that was used in the analytical diffusion calculations.



## 1. Introduction

The creation of helium atoms in metals is very significant, since their precipitation into bubbles can substantially deteriorate the mechanical properties of materials, particularly in metals at high homologous temperatures ($T > 0.5T_m$) where drastic embrittlement due to helium bubble formation at the grain boundary is found [1].

In most of the research on helium–metal interaction, the helium bubbles are induced by implantation [2–4] and tritium decay [5]. The disadvantages of those techniques are the very low near-surface penetration of the helium with a non-homogeneous bubble growth within a depth of a few hundred nanometers for the implantation technique, and the long-term preparation needed for the tritium decay technique. Introduction of helium in metals based on neutron irradiation of aluminum–boron samples [6] was used in this work. The advantage of this technique is the ability to get uniform distribution of helium atoms in the metal. While heating the post-irradiated metal, the helium atoms combine, producing clusters and bubbles. Tiwari and Singh [7] investigated in this way the effect of temperature on the final helium bubble radius in aluminum and copper.

In order to see the formation process of bubbles, in situ observation during heating is needed. Work with in situ ion irradiation of metals in TEM showed a Brownian motion of helium bubbles in the metal [8,9]. But in this case the mechanism of bubble growth and motion is not only a result of the temperature, it is a combination of the irradiation effects and the temperature.

In this paper, we report our investigation of the influence of heating conditions on helium bubble formation and growth in aluminum with $^{10}B$ after neutron irradiation. The helium bubble formation in Al–$^{10}B$ metal was observed in TEM during in situ heating using a hot stage holder. The helium bubbles were formed by heating an Al–$^{10}B$ bulk sample and then prepared for TEM observation in comparison with an in situ heated sample.

## 2. Alloy preparation

Pure aluminum (99.9999%) was melted with 0.15 wt%. $^{10}B$ powder in an arc furnace. The prepared metal was then neutron-irradiated in the Soreq nuclear reactor for 20 h with a flux of $\phi = 3 \times 10^{17}$ [n/m$^2$ s]. The concentration of the helium atoms $N_{He}$ that were created in the bulk of the sample from the reaction $^{10}B + n \rightarrow {}^{7}Li + {}^{4}He$ is given by $N_{He} = \phi\sigma N_{10_B} t = 6.7 \times 10^{23}$ [m$^{-3}$], where $\sigma$ is the cross-section, $N_{10_B}$ is the number of $^{10}B$ atoms per unit volume and $t$ is the irradiation time.

After irradiation the Al–$^{10}B$ alloy was rolled to a 2.7 mm thickness plate. From this plate two groups of specimens were taken:

**Group A** samples were prepared for the in situ TEM observations and investigation of the helium bubble formation and

* Corresponding author. Address: Soreq Nuclear Research Center, Propulsion Physics, Yavne 81800, Israel. Tel.: +972 8 943 4914, mobile: +972 52 850 1508; fax: +972 8 943 4346.
*E-mail addresses:* glam@bgu.ac.il, benny.glam@gmail.com (B. Glam), shalom.elezer@gmail.com (S. Eliezer), dmoreno@netvision.net.il (D. Moreno), dan.eliezer@gmail.com (D. Eliezer).

0022-3115/$ - see front matter © 2009 Elsevier B.V. All rights reserved.
doi:10.1016/j.jnucmat.2009.03.057

growth. The Al–$^{10}$B plate was cut with a low speed saw to obtain 500 μm thickness foils. Disks of 3 mm diameter were punched from the foils and were thinned to 100 μm by grinding. Subsequently, the disks were thinned to produce a hole in their center by an electro-polishing jet in a Tenupol 50 device. The combined procedure of graded grinding and electro-polishing at low temperatures ensures a minimum influence of the preparation procedure on the specimen's microstructure. The estimated thickness of the observed region near the hole, where the electron beam can be transmitted, is about 50–150 nm. The TEM observations were made at different temperatures up to 470 °C.

**Group B** samples were prepared for the bulk diffusion investigation of helium in aluminum. Rolled Al–$^{10}$B bulk samples (2.7 mm thick) were heated to different temperatures and times. TEM characterization was carried out at room temperature.

## 3. Experimental results

### 3.1. In situ observation of bubble formation and growth

The observations were carried out in an FEI T20 model TEM with an acceleration of 200 keV. The group A specimens were heated in discrete steps to 470 °C. At room temperature no helium bubbles were observed except for a restricted strip of 50 nm with a few nanometric bubbles. At 200 °C bubbles started to appear. The bubbles grew, changed their shape, and merged. These processes increased with temperature, while above 400 °C they became faster and the bubble formation front moves toward the Al bulk.

Pictures of TEM selected areas of a specimen heated to 470 °C are shown in Fig. 1. The pictures in Fig. 1(a)–(d) were taken every second. In Fig. 1(a) the bubbles have a faceted shape with typical length of 4–30 nm; $^{10}$B inclusions that did not dissolve in the Al remain, as can be seen at the bottom of the figure. Below them the specimen is thicker and no bubbles were observed. The circle in Fig. 1(a) marks a 50 nm bubble. In Fig. 1(b) the bubble has blown up to 12 small bubbles (~6 nm diameter) that recombine to four bubbles of 15 nm in diameter (Fig. 1(c)) and then to a single 40 nm diameter bubble shown in Fig. 1(d).

Another specimen that was heated to 400 °C is shown in Fig. 2(a). Fig. 2(b) was taken 5 s later at the same temperature. The diagonal line at the bottom right side of the picture is the edge of the sample. The thickness of this area is about 60 nm and increases in thickness as it moves into the bulk. The left area is darker because of this thickness, e.g., it is less transparent to the microscope electrons than the thinner area in the right. The average bubble diameter is ~20 nm. The bubbles at the boundary (bottom right) are larger, about ~50 nm diameter, and have a faceted shape. The two bubbles that are marked with a black circle coalesce to an 80 nm long bubble as shown in Fig. 2(b).

Fig. 3(a)–(d) is from a different selected area of the same specimen. The pictures were taken every minute from Fig. 3(a) to (d). Bubbles 3–30 nm in diameter and various polygonal shapes are shown in Fig. 3(a). During the heating the bubbles' diameter grows, they combine, and change their shape, while new bubbles are created. Bubbles can be observed at different depths, e.g., one above another with partial overlapping. The swelling in the dark at the left side of the pictures in Fig. 3 was caused by accumulation of helium atoms in a grain boundary that were diffused to the bubbles area. During the heating the swelling structure varies and the grain boundary seems to be used as a channel for the helium atoms. New

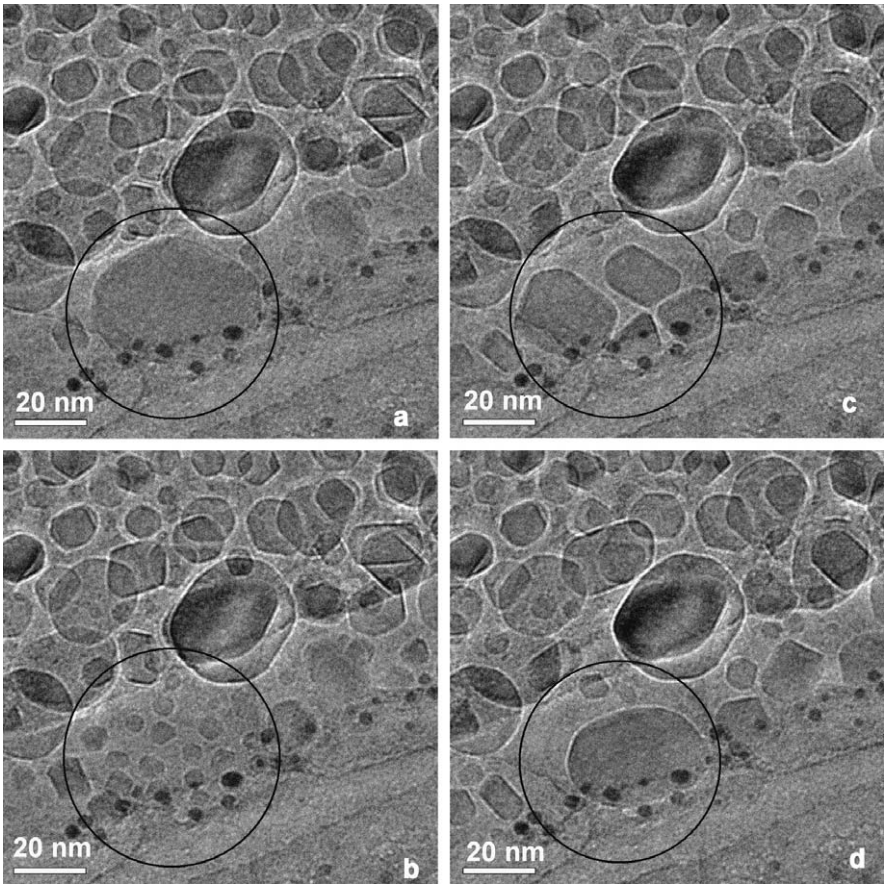


**Fig. 1.** TEM pictures of helium bubble splitting (a and b) and recombination (c and d) after heating to 470 °C in the hot stage.

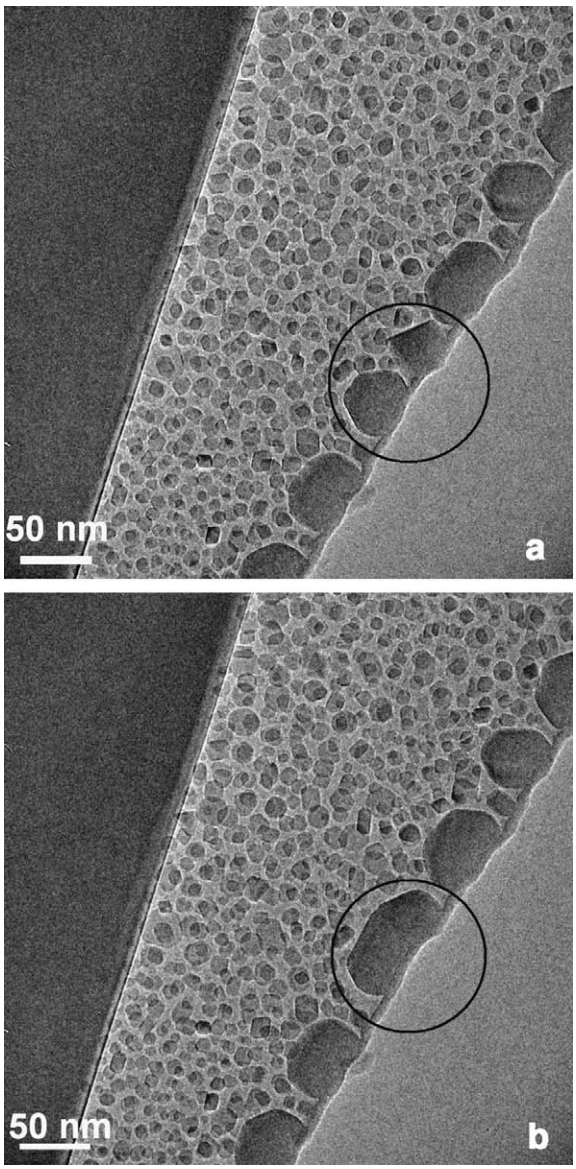


**Fig. 2.** Helium bubble formation and coalescence after heating to 400 °C in the hot stage.

bubbles are formed in the sharp boundary between the bulk (dark region on the left) and the bubble region (brighter on the right). The formation of new bubbles improves the transparence of the material for the electron beam and the brighter area with bubbles becomes wider.

These observations reveal that there is a diffusion of helium from the bulk to the edge. An examination of the specimen with lower magnification as shown in Fig. 4 reveals that the bubbles were created in the area that was exposed to the condensed TEM beam with greater magnifications. In the other areas there is no sign of bubble formation, leading to the conclusion that the electron beam strongly influenced the process.

One of the possible explanations is that the electron beam creates local heating and a temperature gradient in the metal that causes the helium atoms to move to the hotter area by thermal diffusion. This possibility was rejected since calculation of the local heating by the formula suggested by Egerton et al. [10] shows that the temperature rises only by ~1 °C. A radiation damage mechanism that is not accompanied by drastic temperature rise can be caused by displacement of the aluminum atoms due to the bombardment by the TEM energetic electrons. Measurements of the electrons bombard threshold energy made by Pelles and Phillips [11] give a value of 175 ± 25 keV for the aluminum ion displacement. These measurements were obtained with $\sim 5 \times 10^4$ [A/m$^2$] current density. In our experiments we applied a 200 keV electron beam and the current density in the magnification to obtain Figs. 1–4 was $\sim 5 \times 10^4$ [A/m$^2$]. Since it is above the threshold damage found by Pelles and Phillips, we suggest the following explanation for the dependence of helium bubble formation and growth under the electron beam. The bubbles are formed by accumulation of helium atoms in flaw sites. The electron beam in the TEM causes displacement of the aluminum ions and local flaws are used as trap sites for the helium atoms that are moving by diffusion. At room temperature the diffusion rate of the helium in the aluminum is very low and exponentially increases with temperature [12]. Since the diffusion coefficient of helium atoms in aluminum at 400 °C is higher by two orders of magnitude than at room temperature, the helium atoms are moving faster in the metal until they are trapped in the flaws. Bubble formation and growth in these conditions continuously develop in minutes and can be observed in situ by the TEM.

### 3.2. Bubble formation in bulk aluminum

Five samples of 2.7 mm thickness were cut from the irradiated Al–$^{10}$B plate. Each piece was heated to different temperatures for different times as shown in Table 1. After cooling to room temperature, TEM specimens were prepared from each slice and examined to detect helium bubbles. No bubbles were observed in specimens after heating to 400 °C for 50 min, compared to the case of in situ heating where the bubbles formed in seconds at the same temperature. Heating to 500 °C for 50 min (specimen B) also did not reveal any bubbles. The helium bubbles were detected only in the specimens that were heated for longer durations. In specimen C that was heated to 550 °C for 23 h (Fig. 5(a)), the average bubble radius is 5 nm and in specimen D (600 °C for 23 h, the average radius is 10 nm. Heating for 48 h at the same temperature (specimen E, Fig. 5(b))) caused formation of 30 nm radius helium bubbles.

In both cases of heating in the TEM with hot stage and bulk heating, temperature dependence of the helium formation and growth was observed, but the time scale is different: seconds or hours, respectively.

### 3.3. Number of helium atoms in a bubble

The number of helium atoms in a bubble was measured in TEM with an electron energy loss spectrum (EELS) device. According to EELS spectrum, the number of helium atoms in a unit volume is given by

$$N = \frac{I_k}{I_0} \cdot \frac{1}{\sigma_k} \cdot \frac{1}{d}, \tag{1}$$

where $I_k$ is the intensity of the electron loss spectrum at 21.5 eV (first helium ionization energy) and $I_0$ is the intensity of the unscattered electrons, $\sigma_k = 3 \times 10^{-23}$ m$^2$ is the electron cross-section of the appropriate scattered electrons and $d = 70$ nm is the foil thickness in the TEM experiment. An electron intensity spectrum from EELS measurement in a bubble with a radius $r_b = 5$ nm is shown in Fig. 6. Substituting the intensity ratio ($I_k/I_0$), $\sigma_k$, and $d$ into Eq. (1) we get the helium density $N = 4.2 \times 10^{28}$ m$^{-3}$. Multiplying $N$ by the bubble volume, $V_b = (4/3)\,\pi r_b^3$, one gets that in a 5 nm radius bubble there are $N_b = (2.2 \pm 0.2) \times 10^4$ helium atoms.

It is interesting to compare our measurements with the theoretical calculation of helium atoms in a bubble assuming the hard sphere equation of state (EOS) suggested by Brearley and MacInnes [13]:

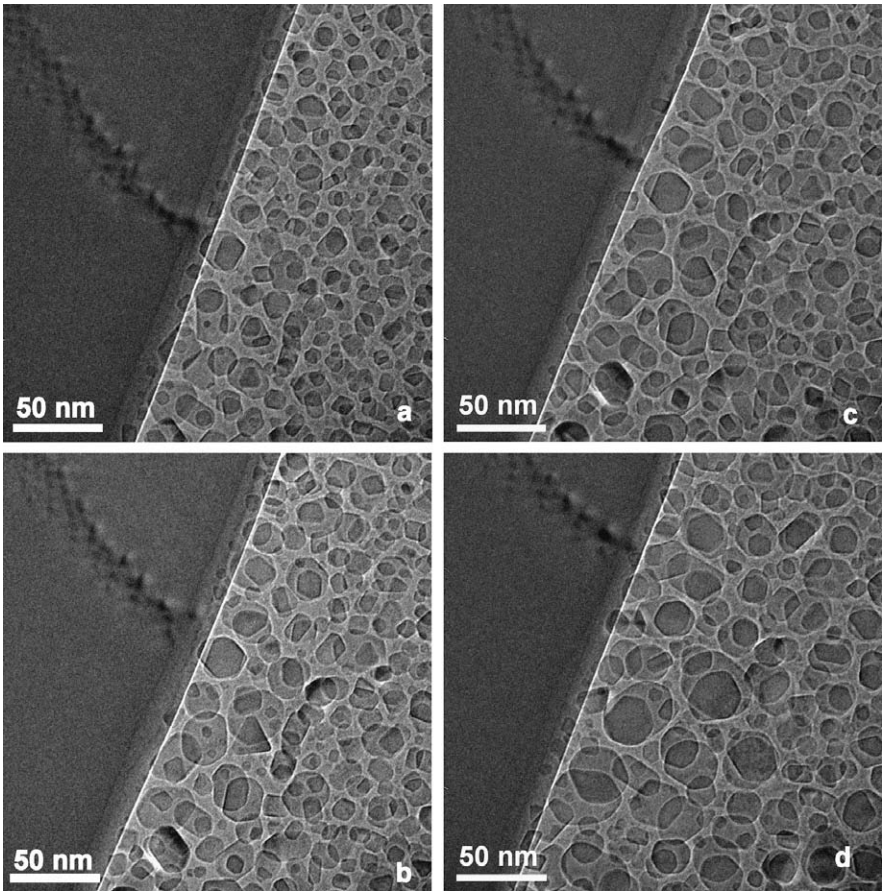


**Fig. 3.** Helium bubble formation and growth after heating to 400 °C in the hot stage. The bubble region expands (from a to d) due to diffusion along the bulk and swelling of the grain boundary.

$$N_b = \frac{P_b V_b}{zkT} = \frac{(2\gamma/r_b)(4/3\pi r_b^3)}{zkT} = \frac{8\pi\gamma r_b^2}{3zkT}, \tag{2}$$

where $P_b$ is the pressure inside the bubble as given by $2\gamma/r_b$ for a bubble radius $r_b$ with a volume $V_b$, and $\gamma = 1\ \mathrm{J/m^2}$ is the aluminum surface tension. $T$ is the temperature, $k$ is Boltzmann's constant, and $z$ is a compressibility factor that is in general a function of temperature and pressure and can be calculated from the Lennard–Jones potential. For a 5 nm radius the helium pressure inside the bubble is 400 MPa. The appropriate compressibility factor for $P_b = 400$ MPa and $T = 300$ K is given by Brearley and MacInnes [13] to be $z = 2.2$. Using $r_b = 5$ nm, $T = 300$ K, and $z = 2.2$ we get a theoretical estimation of $N_b = 2.3 \times 10^4$ helium atoms in the bubble, in excellent agreement with EELS measurements. It is interesting to point out that the agreement between EELS measurement and the theoretical estimate is actually a proof for the correctness of the EOS used for the helium nanoparticle.

## 4. Theoretical estimation of helium bubble formation by diffusion in aluminum: bulk heating and hot stage heating

### 4.1. Bubble formation during bulk heating

In order to understand the experimental results, an analytic approximation of the solution to a diffusion equation with a sink was carried out as follows.

Let us consider a spherical volume with radius $R$. Assuming that the helium atoms are randomly moving in all directions in this volume, the probability $\Gamma$ that helium atoms will pass through a spherical sink with a radius $r$ (as shown in Fig. 7) is given by the relation:

$$\Gamma = d\Omega/4\pi. \tag{3}$$

Under a further assumption that all the atoms that hit the spherical sink will also be trapped inside to create a bubble, the number of helium atoms in the bubble $N_b$ can be evaluated by:

$$N_b = \int_R \int_\Omega (N_{\mathrm{He}} 4\pi R^2 dR)\left(\frac{d\Omega}{4\pi}\right), \tag{4}$$

where $N_{\mathrm{He}}$ is the concentration of helium atoms per unit volume in the aluminum. It is important to emphasize that Eqs. (2) and (4) are independent derivations of $N_b$. Eq. (2) is based on equation of state knowledge of the helium state, while Eq. (4) expresses the diffusion effect with a sink.

For small values of $\theta$ in Fig. 7, $d\Omega = 2\pi r dr/R^2$. Substituting it into Eq. (4) gives:

$$N_b = \pi r_b^2 N_{\mathrm{He}} R. \tag{5}$$

For 3D diffusion, the dependence of the average diffusion distance $R$ in time $t$ is given by $R^2 = 6Dt$. Substituting it into Eq. (5) gives an expression for the bubble growth time:

$$t = \left(\frac{1}{6\pi^2}\right)\left(\frac{N_b}{r_b^2}\right)^2\left(\frac{1}{N_{\mathrm{He}}}\right)^2\left(\frac{1}{D}\right). \tag{6}$$

The diffusion coefficient of helium in aluminum $D$ was taken from Glyde [12] and the number of helium atoms in a bubble $N_b$ can be estimated by the hard sphere EOS (Eq. (2)). Now the diffusion time can be calculated by:

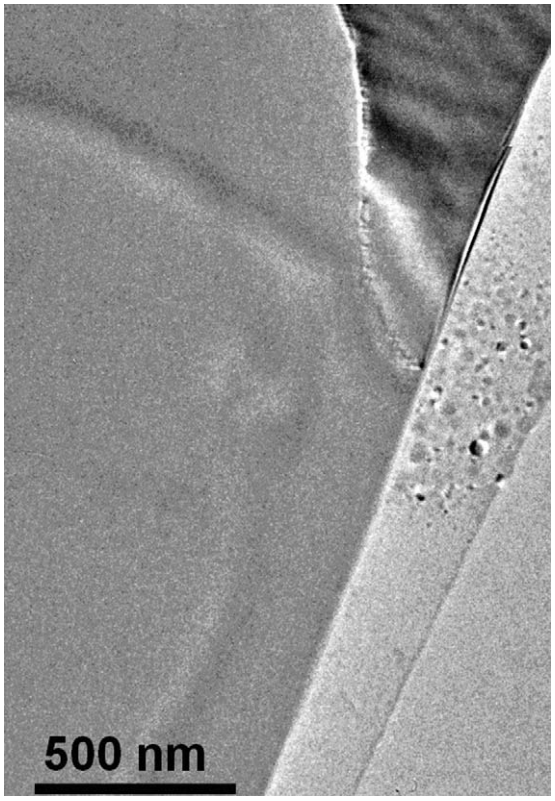


**Fig. 4.** The diagnosed area at low TEM magnification. The bubbles were formed in the restricted area that was subjected to the high magnification electron beam.

**Table 1**
Measurements of helium bubble radii in bulk aluminum after heating to different temperatures.

| Specimen | Heating temperature (°C) | Heating duration (h) | Bubble radius (nm) |
|---|---|---|---|
| A | 400 | 0.8 | Undetectable |
| B | 500 | 0.8 | Undetectable |
| C | 550 | 23 | ~5 |
| D | 600 | 23 | ~10 |
| E | 600 | 48 | ~30 |

$$t = \left(\frac{32}{27}\right)\left(\frac{\gamma}{zkT}\right)^2\left(\frac{1}{N_{\mathrm{He}}}\right)^2\left(\frac{1}{D}\right). \tag{7}$$

Note that since the compressibility factor $z$ is a function of the pressure inside the bubble that is given by $2\gamma/r_b$, the diffusion time is also a function of the bubble radius $r_b$. Fig. 8 represents the bubble radius growth in time as calculated from Eq. (7) for 500 °C, 550 °C, 600 °C, and experimental data from TEM measurements. The theory is in good agreement with the experimental results. The solution reveals a non-linear dependence of the bubble's radius in time and that heating time of several hours is needed for the formation of the smallest helium bubbles that can be observed in the TEM (~3 nm), unlike the case of heating in the hot stage TEM holder.

### 4.2. Bubble formation during heating in the hot stage TEM holder

From the results of the experiments it is clear that helium bubble formation during heating of a TEM specimen in the hot stage holder is faster by orders of magnitude than heating a bulk specimen. The reason is probably the different thicknesses of the heated specimen. A TEM specimen is a round disc with a small hole in its center. The thickness of the diagnosed area changes from a few nanometers near the hole to 100 μm, as shown in Fig. 9. The maximum penetration thickness of the electron beam is ~200 nm.

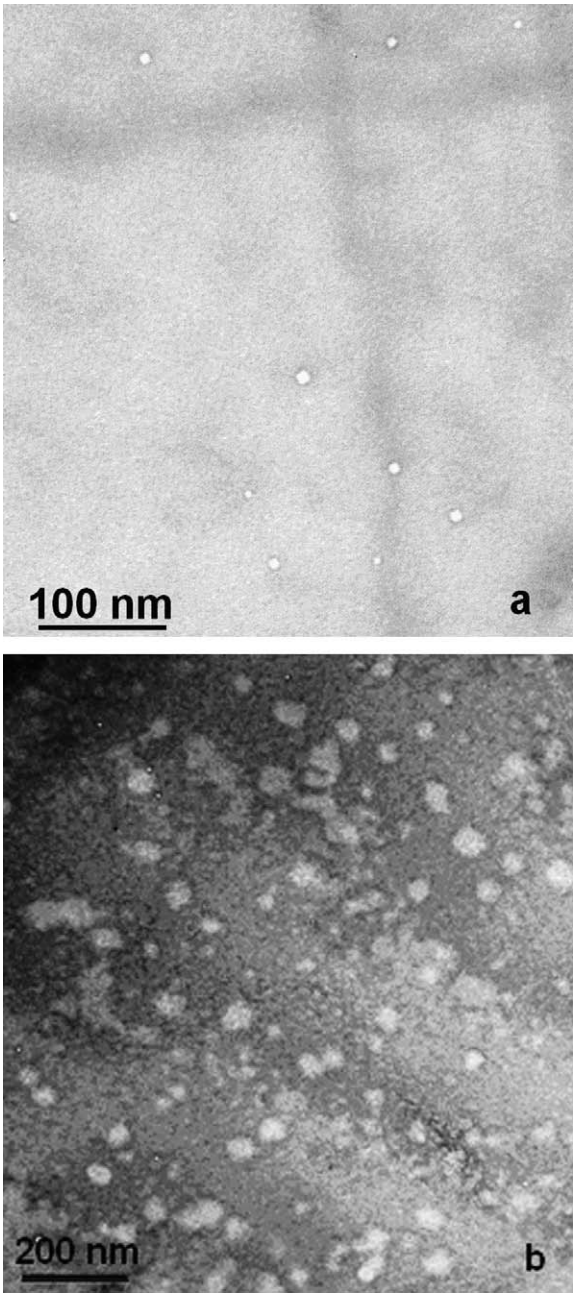


**Fig. 5.** Helium bubble formation after bulk heating to 550 °C for 23 h (a) and to 600 °C for 48 h (b).

From geometric relations, the diffusion distance $L$ of helium atoms from the aluminum to $N$ bubbles can be calculated by:

$$\left(\frac{1}{2}\right)N_{\mathrm{He}}\left(\frac{d}{2}\right)\left(\frac{\pi L^2}{2}\right) = N_b N \rightarrow L = \sqrt{\frac{8N_b N}{\pi N_{\mathrm{He}} d}}. \tag{8}$$

Substituting Eq. (8) for the expression for the average diffusion distance $L = \sqrt{6Dt}$ will give an expression for the diffusion time of helium in aluminum while heating it in the hot stage holder:

$$t = \frac{4}{3\pi}\frac{N_b N}{N_{\mathrm{He}}}\frac{1}{Dd}. \tag{9}$$

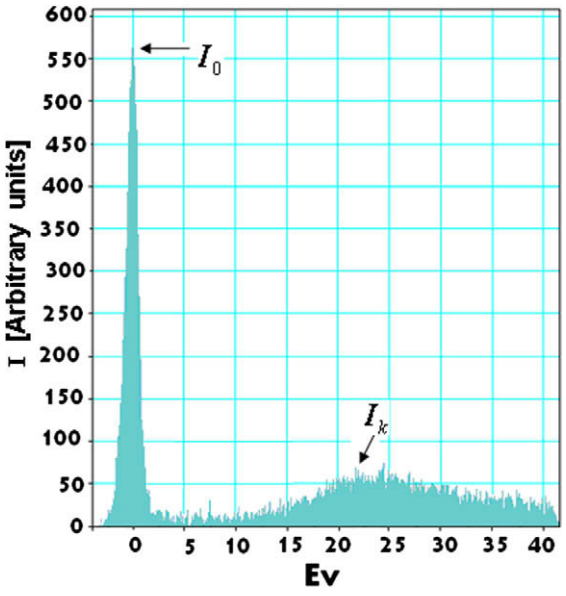


**Fig. 6.** Electron energy loss spectrum (EELS) measurements in 5 nm helium bubble.

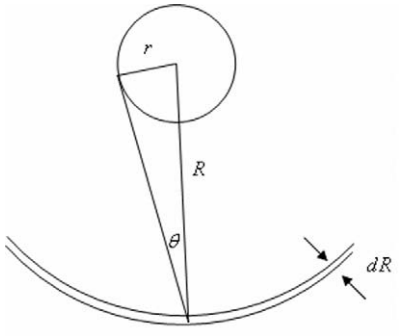


**Fig. 7.** Schematic description of helium atom diffusion and trapping in a sink.

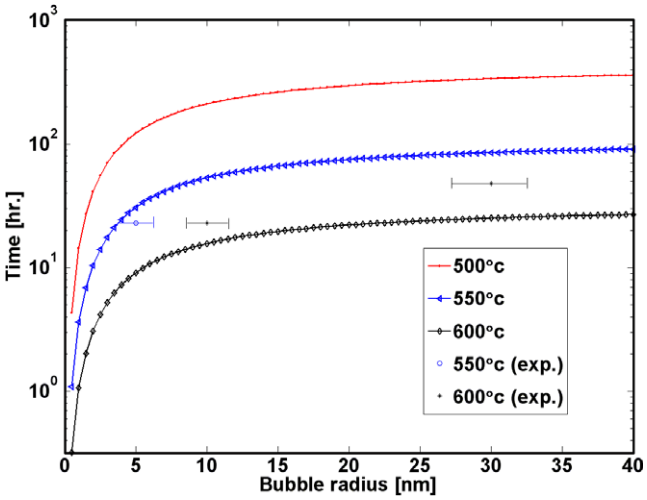


**Fig. 8.** Time for helium bubble growth in bulk aluminum at different temperatures, calculated and experimental.

In Fig. 10 one can see helium bubbles that were formed during heating to 400 °C in the hot stage holder. The dashed line represents the boundary of the bubble region as observed one minute before. During this minute about $N \approx 130$ new bubbles with

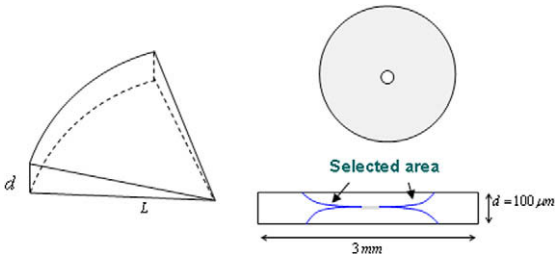


**Fig. 9.** Scheme of TEM specimen.

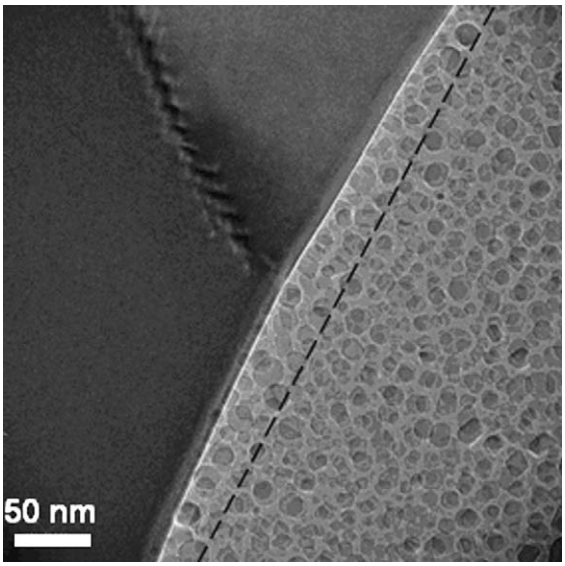


**Fig. 10.** TEM picture of the helium bubble region after heating to 400 °C in the hot stage. The dashed line denotes the boundary of the helium bubble region as observed 1 min before. (For interpretation of the references to colour in this figure legend, the reader is referred to the web version of this article.)

8 nm average radius were formed. From the hard sphere EOS the calculated number of helium atoms in one bubble is $N_b \approx 6.5 \times 10^4$. At 400 °C the coefficient of helium diffusion in aluminum is $D \approx (8.9 \pm 8) \times 10^{-16}$ [m$^2$/s]. At these conditions the calculated diffusion time (from Eq. (9)) is 60 s, in very good agreement with the experimental results.

## 5. Conclusions

Helium bubble formation in aluminum was investigated experimentally and analytically. The formation and growth process was observed in situ when heating the metal in TEM with a hot stage holder. It was found that the electron beam in the TEM influences the process and the time scale for bubble formation is seconds. Further TEM observations at room temperature of post-heated bulk aluminum reveal that the time for bubble formation in this case is hours. Analytical calculations of the diffusion time for bubble formation in both of the cases explain the experimental results. The number of helium atoms in a bubble was calculated from EELS measurements. These measurements confirm the hard sphere EOS that was used for the diffusion calculations.

## Acknowledgements

The authors would like to thank Dr Yaron Kauffmann for mastering the TEM and Dr Michael Aizenshtein for his metallurgical help. This work was supported by the joint VATAT-IAEC common lab foundation.

## References

[1] H. Trinkaus, B.N. Singh, J. Nucl. Mater. 323 (2003) 229.
[2] J. Marian, B.D. Wirth, J.M. Perlado, Phys. Rev. Lett. 88 (2002) 255507.
[3] A.J.E. Foeman, B.N. Singh, J. Nucl. Mater. 133&134 (1985) 451.
[4] D. Moreno, D. Eliezer, Scripta Mater. 35 (1996) 1385.
[5] M. Satou, H. Koide, A. Hasegawa, K. Abe, H. Kayano, H. Matsui, J. Nucl. Mater. 234 (1996) 447.
[6] S.R. Pati, P. Barrand, J. Nucl. Mater. 31 (1969) 117.
[7] G.P. Tiwari, J. Singh, J. Nucl. Mater. 172 (1990) 114.
[8] K. Ono, K. Arakawa, K. Hojou, M. Oohasi, R.C. Birtcher, S.E. Donnelly, J. Electron Microsc. 51 (2002) 245.
[9] K. Ono, S. Furuno, K. Hojou, T. Kino, K. Izui, O. Takaoka, N. Kubo, K. Mizuno, K. Ito, J. Nucl. Mater. 191–194 (1992) 1269.
[10] R.F. Egerton, P. Li, M. Malac, Micron 35 (2004) 399.
[11] G.P. Pelles, D.C. Phillips, J. Nucl. Mater. 80 (1979) 207.
[12] H.R. Glyde, K.L. Mayne, J. Nucl. Mater. 15 (1965) 997.
[13] I.R. Brearley, D.A. MacInnes, J. Nucl. Mater. 95 (1980) 239.